JGR Biogeosciences

RESEARCH ARTICLE
10.1029/2020JG005737

Biogeochemical and Hydrological Variables Synergistically Influence Nitrate Variability in Coastal Deltaic Wetlands

Alicia Sendrowski[1,2], Edward Castañeda-Moya[3,4], Robert Twilley[4], and Paola Passalacqua[2]

[1]Department of Geosciences, Colorado State University, Fort Collins, CO, USA, [2]Department of Civil, Architectural, and Environmental Engineering, Center for Water and the Environment, Austin, TX, USA, [3]Now at Southeast Environmental Research Center, Institute of Environment, Florida International University, Miami, FL, USA, [4]Department of Oceanography and Coastal Sciences, College of the Coast and the Environment, Louisiana State University, Baton Rouge, LA, USA

Key Points:

- We measure how hydrological and biogeochemical controls influence nitrate fluctuations in delta wetlands by classifying variable interaction
- Wetland variables work together (act synergistically) to influence nitrate variability
- Nitrate variability is controlled by variation in vegetation density and external driver forcing

Correspondence to:
P. Passalacqua,
paola@austin.utexas.edu

Citation:
Sendrowski, A., Castañeda-Moya, E., Twilley, R., & Passalacqua, P. (2021). Biogeochemical and hydrological variables synergistically influence nitrate variability in coastal deltaic wetlands. *Journal of Geophysical Research: Biogeosciences*, *126*, e2020JG005737. https://doi.org/10.1029/2020JG005737

Received 10 MAR 2020
Accepted 9 AUG 2021

Author Contributions:
Conceptualization: Alicia Sendrowski, Paola Passalacqua
Data curation: Edward Castañeda-Moya
Formal analysis: Alicia Sendrowski
Funding acquisition: Robert Twilley, Paola Passalacqua
Investigation: Alicia Sendrowski, Edward Castañeda-Moya, Paola Passalacqua
Resources: Edward Castañeda-Moya, Robert Twilley
Writing – original draft: Alicia Sendrowski, Paola Passalacqua
Writing – review & editing: Alicia Sendrowski, Edward Castañeda-Moya, Robert Twilley, Paola Passalacqua

Abstract Coastal river deltas are centers of surface water nitrate processing, yet the mechanisms controlling spatio-temporal patterns in nutrient variability are still little understood. Nitrate fluctuations in these systems are controlled by complex interactions between hydrological and biogeochemical drivers, which act together to transport and transform inorganic nutrients. Distinguishing the contributions of these drivers and identifying wetland zones where nitrate processing is occurring can be difficult, yet is critical to make assessments of nutrient removal capacity in deltaic wetlands. To address these issues, we analyze relationships among regional "external" (river discharge, tides, wind) and local "internal" (water level, temperature, turbidity, and nitrate) variables in a deltaic wetland in coastal Louisiana by coupling a process connectivity framework with information theory measures. We classify variable interactions according to whether they work uniquely, redundantly, or synergistically to influence nitrate dynamics and identify timescales of interaction. We find that external drivers work together to influence nitrate transport. Patterns of hydrological and sediment connectivity change over time due to tidal flushing and discharge variation. This connectivity influences the emergence of functional zones where local nitrate fluctuations and temperature and water level process couplings are strong controls on nitrate variability. High vegetation density decreases hydrological process connectivity, even during periods of high river discharge, but it also increases biogeochemical process connections, due to the lengthening of the hydraulic residence time. Based on these results we make recommendations for monitoring nitrate in a wetland.

Plain Language Summary With nitrate export to oceans expected to increase in the coming decades, river deltas will serve as an increasingly important site at continental margins for processing nitrate. It will be critical to understand the drivers of nitrate variability and identify locations of enhanced processing. We use information theory to quantify the process connectivity among regional hydrological and local biogeochemical controls on nitrate in a wetland in Louisiana. We find that river discharge fluctuations, tidal flushing, and vegetation density affect the hydrological connectivity of the wetland that governs the strength of hydrological and biogeochemical influences on nitrate. This study reveals the mechanisms that influence nitrate transport and transformation, which may be used to design monitoring studies and aid coastal restoration projects.

1. Introduction

Deltaic wetlands are critical coastal environments that can serve as the final processing center for nutrients before export to the ocean. A main research area for wetlands is their nitrate removal capacity, given that nitrate is considered a contaminant of concern in watersheds and the coastal zone. Nitrate loading in aquatic systems has been linked to eutrophication (Rabalais et al., 2009; Turner & Rabalais, 1994) and hypoxia (Diaz & Rosenberg, 2008; Selman et al., 2008; Turner et al., 2008) resulting in significant ecological and economic losses in places such as the lower Mississippi River Basin and the Gulf of Mexico. Despite insights into nitrate removal mechanisms such as denitrification, plant uptake, and burial (Bowden, 1987; Kadlec, 2010, 2012; Reddy et al., 1984; Rivera-Monroy et al., 2010) and their influences

(e.g., land use [Hansen et al., 2018], loading rate [Mitsch et al., 2005; Mulholland et al., 2008], inflow [Lane et al., 1999, 2003], temperature [Kadlec, 2010], and soil composition [Vanzomeren et al., 2013]), there is a lack of understanding of the spatial and seasonal patterns of nitrate variability in coastal deltaic wetlands (Henry & Twilley, 2014; S. Li et al., 2020; Shaheen et al., 2016; Twilley et al., 2019) due to the complex interactions among hydrology, geomorphology, and biogeochemistry that control nitrate processing. These dynamics include the heterogeneous hydrological and biogeochemical processes taking place within wetlands (conceptualized as local or internal wetland processes) and the exchanges taking place between wetlands and the surrounding landscape (i.e., regional or external processes that aid in the delivery of material into wetlands). Further knowledge of the processes that influence nitrate transport and transformation would benefit nutrient modelers and land use managers aiming to make informed decisions on monitoring and restoration programs in coastal wetlands. In this work, we analyze the internal and external controls on nitrate variability in a deltaic wetland in coastal Louisiana.

External drivers, such as river discharge, tides, and wind, can affect timescales and magnitudes of nitrate transport into wetlands (Caffrey & Day, 1986; Lane et al., 2011), while internal drivers, such as water level, sediment, temperature, and nutrients, can control reaction rates related to nitrate transformation (Bowden, 1987; Kadlec, 2010). Their interaction influences wetland functioning such that flow through wetlands may result in the formation of "functional zones" of nitrate processing (Burt & Pinay, 2005) where variables across space interact to alter nutrients. These functional zones may be related to spatial differences in soil elevation along the intertidal profile that determine distinct hydrogeomorphic (HGM) zones in wetlands associated with deltaic floodplains (Bevington & Twilley, 2018; Twilley et al., 2019). These zones are characterized by distinct hydroperiod, sediment organic matter content, and vegetation communities, with zonation and composition controlled by the elevation gradient and interspecific competition (Bevington & Twilley, 2018; Carle & Sasser, 2016; Shaffer et al., 1992). Individual locations within HGM zones (e.g., vegetation patches) along the elevation gradient can serve as "hotspots" of nitrate influence (McClain et al., 2003) by locally reducing flow velocity and increasing contact time at the soil-water interface.

The complex flow patterns in deltaic wetlands that form hotspots and functional zones can be conceptualized using a hydrological connectivity framework which describes the water-mediated transport of mass and energy among different landscape components (Bracken & Croke, 2007; Bracken et al., 2013; Tetzlaff et al., 2007). Nitrate fluctuations in these systems are governed by the information exchanged between system drivers and response variables, referred to as process connectivity (Passalacqua, 2017; Ruddell & Kumar, 2009a, 2009b). This process connectivity is influenced by the static physical links between locations in a wetland (referred to as structural connectivity) and the dynamic links of fluxes across space (functional connectivity [Lexartza-Artza & Wainwright, 2009]). Using connectivity concepts, a deltaic wetland can be represented as a network of interacting variables, that is, important information about processes is conveyed such that uncertainty in a variable is reduced. However, the dependencies among system variables can make it difficult to identify how variables contribute to nitrate fluctuations. For example, a variable may influence nitrate variability independently of any other variable (i.e., be a unique influence on nitrate), may act with another variable to influence nitrate (i.e., synergize to influence nitrate), or could influence nitrate similarly to another variable (i.e., synchronize or be redundant with that variable). To better understand the controls on nitrate variability across a wetland requires an approach that can classify these process connections and distinguish the locations that form hotspots and functional zones.

Quantitative measures of information theory (IT) (Shannon, 1948) provide an approach to distinguish variable interactions. IT is mathematics that uses the probability density function of variables to track the flow of information among variables. Previous applications of IT in deltaic landscapes have quantified the influence of external drivers on delta water levels, identifying distinct timescales and magnitudes of tidal, riverine, and wind forcing (Sendrowski & Passalacqua, 2017). Dependencies among variables can be measured for any number of multivariate interactions. A particular form of IT, referred to as information partitioning, can be used to quantify relationships among three variables. Using this approach, we can classify relationships into unique (two variables independently influence another variable), synergistic (two variables jointly influence a variable), and redundant (two variables similarly influence another variable) (Goodwell & Kumar, 2017a, 2017b; Williams & Beer, 2010, 2011).

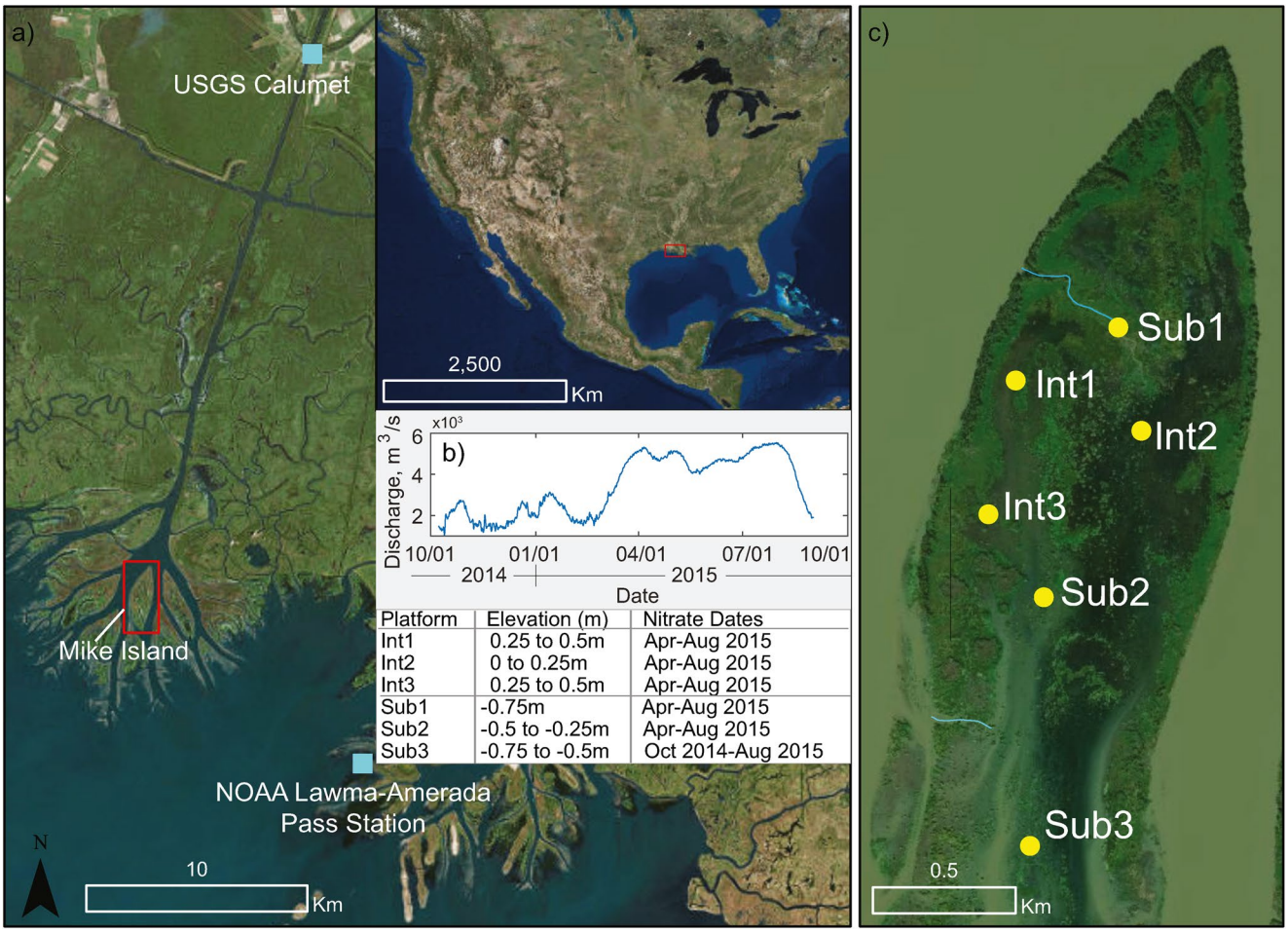

Figure 1. Study area and measurement locations. (a) Map of the Wax Lake Delta (WLD) (left) and the Atchafalaya Delta (right). Squares show the measurement locations of discharge, tides, and wind. Inset shows location of this system in the U.S. (b) Discharge measured at the (USGS) Calumet Gauge located 17 km upstream of WLD for the period encompassing nitrate measurements (October 2014–August 2015). (c) Map of Mike Island showing the location of the six platforms used in this study. Lines show secondary channels connecting the distributary channel and island interior. Images from the US Geological Survey. Inset table shows the surface elevation of the platform location (in NAVD88 [m]) and the dates of nitrate measurement for each platform.

Previous approaches to understand nitrate variability and wetland dynamics include the formation of system budgets that track flows of water, solids, and solutes, and inform on the sources, residence time, and removal efficiencies of nutrients (Boynton et al., 2008; Hyfield et al., 2008; Lane et al., 2003). However, only tracking mass inflows and outflows can be very site specific and therefore hard to extrapolate across new areas and may also obscure or overlook important processes that occur at a different scale. We address these issues by forming a budget of system linkages—we track the relationships (process couplings) that influence nitrate over time and space rather than tracking mass. By mapping the network of relationships that compose nitrate processing, we can gain insights into dynamics that likely occur in many systems.

Our focus area for this work is Mike Island in the Wax Lake Delta (WLD) in coastal Louisiana (Figure 1). Using variables measured at various locations within this site coupled with observations of external drivers (described in Section 2), we analyze hydrological and biogeochemical controls on nitrate fluctuations and distinguish the unique, synergistic, and redundant relationships of different drivers using information partitioning (Section 3). We discuss the mechanisms affecting wetland process connections across hydrogeomorphic zones over time and make recommendations for monitoring nitrate in a wetland (Section 4).

2. Materials and Methods

2.1. Site Description and Data Collection

WLD is a ~100 km^2 actively prograding river delta in coastal Louisiana with a median discharge of 3,000 m^3s^{-1} and a tidal range of 30 cm. The delta is characterized by elongated arrow-shaped islands with subtidal interdistributary bays surrounded by narrow higher elevation levees. The interdistributary bays widen and deepen in the downstream direction, and have a deeper trough down the center (Bevington et al., 2017; Shaw et al., 2016). The islands extend 6 km sub-aerially and another 5–10 km sub-aqueously (Bevington & Twilley, 2018; Shaw et al., 2013, 2016). The deltaic wetlands are composed of mineral sediments that are colonized by woody, shrub, and herbaceous fresh marsh species. Vegetation zonation and species composition are mainly controlled by soil elevation (Carle & Sasser, 2016); black willow trees (*Salix nigra*) and elephant ear (*Colocasia esculenta*) dominate island tops and margins, while American lotus (*Nelumbo lutea*) and submerged aquatic vegetation populate central and downstream regions of the islands (lower elevation). Vegetation in WLD has a seasonal signature; studies using the normalized difference vegetation index applied to delta imagery from 1984 to 2015 find peak and minimum biomass to occur in August–October and January–February, respectively (Olliver & Edmonds, 2017). Cold fronts and tropical storms influence vegetation and water and sediment fluxes in this region (Bevington et al., 2017; Carle & Sasser, 2016).

Fluxes enter Mike Island through large secondary channels and flow over subaqueous levees resulting in high structural and functional connectivity within the island. The distributary channel adjacent to Mike Island loses up to 27% of its flow moving downstream (Hiatt & Passalacqua, 2015). Hydrological connectivity on the island is mediated by vegetation density (Hiatt & Passalacqua, 2017; Wright et al., 2018) and seasonality, resulting in spatial variability in water exposure times (Christensen et al., 2020; Hiatt et al., 2018). Based on numerical experiments, the system-wide median exposure time (amount of time a water parcel spends in a domain of interest) is 10 h regardless of incoming river discharge or tidal conditions (Hiatt & Passalacqua, 2017; Hiatt et al., 2018) and field experiments have shown longer timescales on the order of days (Hiatt & Passalacqua, 2015).

The delta shows enhanced nitrate processing (Henry & Twilley, 2014; Hiatt et al., 2018; S. Li et al., 2020) making it a suitable site to measure hydrological and biogeochemical controls on surface water nitrate dynamics. To capture constituent variability across the island, six permanent telemetry platforms were installed during January and February 2014. After mapping the HGM zones of the delta based on field observations and vegetation surveys under different hydrological conditions (Bevington & Twilley, 2018), these instrument platforms were placed in two HGM zones (Intertidal [Int] and Subtidal [Sub]) where previous monitoring results from fixed stations on Mike Island suggested that water flow was distinct in the central distributary trough (Subtidal) compared to the intertidal zones along the edges of the island. Three platforms (Sub1, Sub2, Sub3) were located along the longitudinal gradient from upstream to downstream in the interdistributary trough; two (Int1 and Int3) in the western side of Mike Island, and one in the eastern side (Int2; Figure 1). Additionally, platform Sub1 was deployed at the end of a secondary channel, and Int1, 2, and 3 in locations of denser vegetation and higher elevation (Figure 1c). Each platform was equipped with sensors that registered continuous measurements of water depth (pressure transducer; Campbell Scientific), temperature and conductivity (Campbell Scientific), and turbidity (OBS-500; Campbell Scientific). Surface water nitrate concentrations were measured using submersible ultraviolet nitrate analyzers (SUNA V2; chemical free sensor, Satlantic). All sensors were installed 17.8 cm above the bed. Measurements of nitrate began at location Sub3 (Figure 1c) in October 2014, while the other five stations recorded data starting in April 2015. All data collection continued until August 2015. Data from all sensors were recorded at one-hour intervals and stored in a CR-1000 Datalogger (Campbell Scientific) in each platform. For the nitrate data, hourly data consisted of an average of the previous 30s. Measurements of discharge were collected from the US Geological Survey (USGS) Calumet Gauge (#07381590), located 17 km upstream of WLD. Tide and wind data were collected from the National Oceanic and Atmospheric Administration (NOAA) Lawma Amerada Pass station (#8764227), located 10 km east of WLD in the Atchafalaya Delta.

2.2. Data Processing

Prior to analysis, the discharge and wind time series were low-pass filtered to remove high frequency (sub-daily) fluctuations (Sendrowski & Passalacqua, 2017). The wind speed and direction were also combined into a single series by multiplying the negative wind speed by the cosine of the wind direction resulting in a North–South (N–S) oriented wind signal. Analysis with an East–West signal revealed similar dependencies to the N–S signal for this system. We combined the speed and direction as previous studies suggest that directional winds display stronger influences on fluxes in coastal Louisiana compared to speed or direction alone (Geleynse et al., 2015; C. Li et al., 2011).

If sensors became subaerial, observations of water level, turbidity, and nitrate concentration were set to zero, while temperature values were discarded. We corrected water depth measurements for atmospheric pressure and sensor height above bed; we refer to this local water depth as water level for the rest of this study. Turbidity observations spanned a large range of values. We performed a sensitivity analysis to determine a threshold that did not remove any variable dependencies with turbidity. After this analysis, we chose a threshold of 900NTU; any measurements above this level were discarded. To avoid gap filling and indirectly adding spurious dependencies in the data (Smirnov, 2013), variables that had more than 10% of their data missing for the period of interest were not analyzed.

2.3. Information Theory Statistics

IT measures are quantified using the probability density function of variables. If X is the variable or signal of interest, the uncertainty contained within that variable can be quantified using the Shannon entropy:

$$H(X) = -\sum_{i=1}^{N} p(x_i) log_2[p(x_i)] \tag{1}$$

where x_i is an outcome of X and $p(x_i)$ is the probability of that outcome. The units of $H(X)$ depend on the base of the logarithm; here, we use base 2, thus $H(X)$ is measured in bits.

Information flow (from a source or multiple sources) results in the reduction in uncertainty of a target variable (Ruddell & Kumar, 2009a). Interactions between two variables (a source and a target) are based on the joint probability distribution. The mutual information (MI) quantifies the shared information between two variables, X (target) and Y (source), and is shown here in terms of the Shannon entropy of X and Y, which is a measure of the reduction in uncertainty of X when Y is known (second expression on RHS):

$$MI(X;Y) = H(X) + H(Y) - H(X,Y) = H(X) - H(X \mid Y) \tag{2}$$

MI is a symmetric measure and also represents a reduction in uncertainty of Y when X is known, thus the choice of source or target is arbitrary. However, MI can be quantified over a time lag (τ) and stated in terms of the probability distributions of X and Y:

$$MI(X_\tau,Y) = \sum_{x_{t-\tau},y_t} p(x_{t-\tau},y_t) log_2 \frac{p(x_{t-\tau},y_t)}{p(x_t)p(y_t)} \tag{3}$$

where $p(x_{t-\tau},y_t)$ is the joint probability of lagged-X and Y. These lagged MI values can be different depending on which is the source or target. Here, we identify the lag at maximum MI as the timescale of interaction. MI can also be extended for three interacting variables (multiple sources (Y and Z) on a target [X]):

$$MI(X;Y,Z) = \sum_{x,y,z} p(x,y,z) log_2 \frac{p(x,y,z)}{p(x)p(y,z)} \tag{4}$$

$$MI(X;Y,Z) = MI(X;Z) + MI(X;Y \mid Z) = H(X) - H(X \mid Y,Z) \tag{5}$$

The first expression on the RHS of Equation 5 states that the shared information that Y and Z provide to X can be partitioned into the information Z provides to X and the additional information Y provides to X when Z is known. In terms of the Shannon entropy (second expression on the RHS), the reduction in uncertainty of X is dependent on the interaction between Y and Z. Two sources can influence X in three ways: (a) uniquely (U), Y and Z are independent and provide distinct information about X, (b) redundantly (R), Y

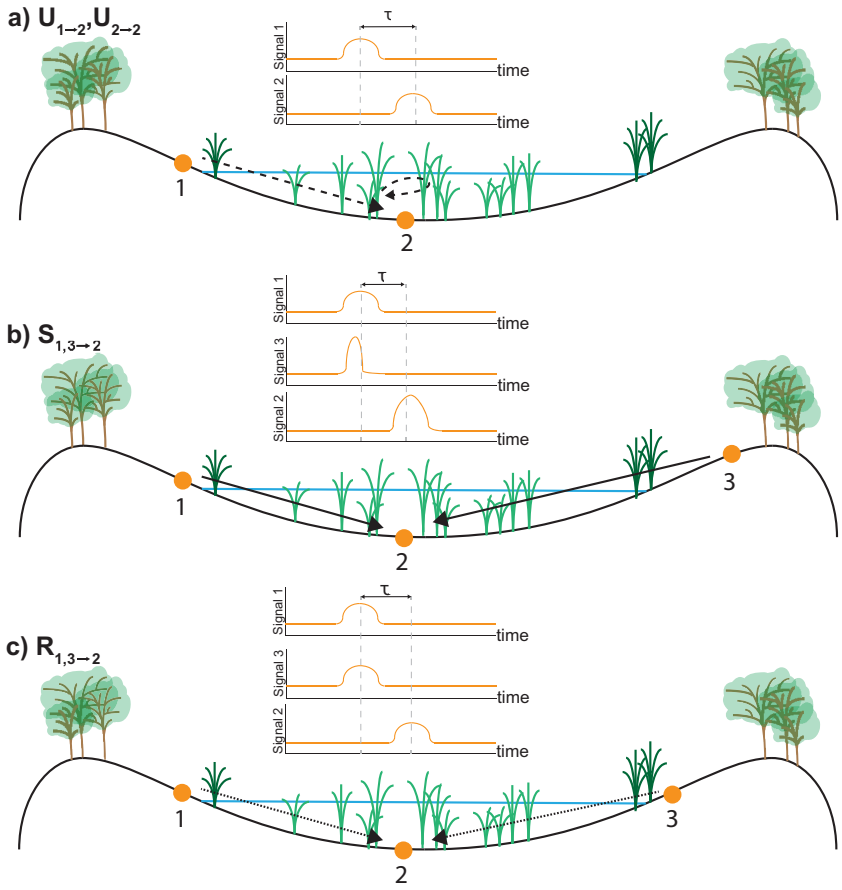

Figure 2. Conceptual figure showing examples of strong (a) U, (b) S, and (c) R relationships in a wetland complex. Variable 2 is the target while 1 and 3 are sources. Each component shows example time series that result in high values of U, S, and R. The strongest dependencies occur at time lag τ. Notation for each relationship shows the sources in the subscript on the left and targets on the right, that is, $S_{1,3\rightarrow 2}$ is the synergistic interaction of 1 and 3 that influences 2.

and Z provide the same information about X, and (c) synergistically (S), Y and Z work together to influence X (Goodwell & Kumar, 2017a, 2017b; Goodwell et al., 2018; Williams & Beer, 2010, 2011):

$$MI(X;Y,Z) = U_1(X;Y) + U_2(X;Z) + R(X;Y,Z) + S(X;Y,Z) \tag{6}$$

Thus, the reduction in uncertainty of X from interaction with Y and Z can be classified according to the interaction of Y and Z. This classification is referred to as partial information decomposition (Williams & Beer, 2010, 2011). Considering these components, MI for the individual source-target pairs can be restated from Equation 2 as follows:

$$MI(X;Y) = U_1(X;Y) + R(X;Y,Z) \tag{7}$$

$$MI(X;Z) = U_2(X;Z) + R(X;Y,Z) \tag{8}$$

where the information of a single source influencing a target is the sum of the unique influence from that source and the redundant information provided by the two sources Y and Z. In this analysis, Equations 6–8 are used to compute U, R, and S for the interaction of X, Y, and Z in addition to another measure that takes into account the upper and lower bound of redundancy and the dependency between sources, called the rescaled redundancy. For more information on this measure, information partitioning, and an expanded discussion of the statistics, we refer to Goodwell and Kumar (2017a, 2017b).

As an example of the above components, we show examples of strong U, S, and R relationships for three signals in an idealized cross-section of a wetland complex (Figure 2). We focus on a variable measured at

three locations, where the variable at location 2 is the target and 1 and 3 are sources. Example variables include water level, sediment concentration, or nutrient concentration. Notation for U, R, and S relationships follows $U_{\text{source}\rightarrow\text{target}}$, $R_{\text{source1,source2}\rightarrow\text{target}}$, and $S_{\text{source1,source2}\rightarrow\text{target}}$, respectively. High U values are measured when the variable at 1 contains distinct information that influences location 2 (i.e., transport occurs from 1 to 2, $U_{1\rightarrow2}$). This dependency is strongest at time lag τ (Figure 2a). High U may also occur for a variable influencing itself (i.e., $U_{2\rightarrow2}$, similar to an autocorrelation, rounded arrow in Figure 2a). High S values are measured when the variables at 1 and 3 influence 2 due to transport occurring from these locations to 2 but there is no transport between them ($S_{1,3\rightarrow2}$, Figure 2b). High S could also result from processes at 1 and 3 that occur together at 2, thus 1 and 3 inform on 2 beyond a linear sum of signals. Finally, high R values are measured when 1 and 3 are strongly synchronized due to direct transport between 1 and 3, or 1 and 3 are similarly influenced by the same process but are not directly connected, such that they similarly influence 2 (Figure 2c). U, R, and S couplings therefore encompass physical flow in the system (i.e., mass movement across space, a result of flow paths specific to the wetland), biogeochemical "flow" (reactions occurring among variables at a single location), and information flow (variables have information about a process that informs (reduces uncertainty) on another variable that may be physically disconnected).

2.4. Experimental Design

We aim to measure (a) the overall process connectivity of Mike Island, (b) the controls on nitrate variability, and (c) the hotspots and functional zones that influence nitrate processing. To accomplish these goals, we quantify information partitioning among variables using data measured from (a) October 2014 to August 2015 (referred to as the Oct to Aug dataset) and (b) April to August 2015 (referred to as the Apr to Aug data set). The second data set includes the additional nitrate measurements that began in April 2015. We use a sliding window to capture variability over time; both data sets are partitioned into 21-day windows with each window shifted by one day, totaling 306 and 131 windows for the Oct–Aug and the Apr–Aug data sets, respectively. A length of 21 days captures submonthly fluctuations of island constituents and also ensures sufficient data to create representative probability distributions using fixed interval binning for the calculation of variable dependencies (Ruddell & Kumar, 2009a).

We use the software from Goodwell and Kumar (2017a, 2017b) to calculate U, R, and S among all possible variable combinations for every window. Statistical significance is determined using the shuffled surrogates method; all time series observations in both datasets are randomly shuffled to destroy time dependencies. U, R, and S are then recalculated for all relationships using these random series. This procedure is done many times to generate a distribution of random U, R, and S values. Relationships are statistically significant at a 95% confidence level if the original U, R, and S values exceed a certain threshold determined using a one-tailed hypothesis test. Significant relationships are visualized using process networks (Figure 3).

While we lack specific information on the vegetation distribution of Mike Island during the study period, we capture its influence by exploring relationships seasonally in the first two analyses. The season begins when the window shifts to include the start of the season (i.e., the spring season begins when a window contains data from March 20). Fall contains windows covering October–December, winter: December–March, spring: March–June, and summer: June–August. Based on previous analysis of the consistent patterns of vegetation coverage (Olliver & Edmonds, 2017), we assume that peak biomass (maximum vegetative drag) occurs in the late summer/fall and minimum biomass occurs in the winter of our study period.

In our first analysis, both data sets are used to explore the connectivity of Mike Island by measuring the spatial dependencies of water level, turbidity, and nitrate (Figure 3a). We focus on relationships within the same variable and compute U, R, and S information among the six locations. U information is measured between all possible location pairs (e.g., for water level [WL], we calculate the influence of Sub1-WL on Int1-, Int2-, Int3-, Sub1-, Sub2-, and Sub3-WL, of Int1-WL on all WL ($U_{\text{Int1-WL}\rightarrow\text{WL}}$, etc.) resulting in 36 U relationships for each variable for each window. We partition these relationships and show the proportion of self (e.g., $U_{\text{Sub1}\rightarrow\text{Sub1}}$) and non-self (e.g., $U_{\text{Sub1}\rightarrow\text{Int1}}$, $U_{\text{Sub1}\rightarrow\text{Int2}}$) couplings. For R and S information, we measure the influence of all possible spatial couplings (e.g., for WL, we calculate the $R[S]$ information provided by Sub1-and Int1-WL to all WL ($R[S]_{\text{Sub1,Int1-WL}\rightarrow\text{WL}}$, by Sub1-and Int2-WL to all WL ($R[S]_{\text{Sub1,Int2-WL}\rightarrow\text{WL}}$, etc.) resulting in 90 R and 90 S relationships for each variable for each window. We partition these couplings and show the proportion of $R(S)$ relationships that result from couplings among subtidal (lower elevation

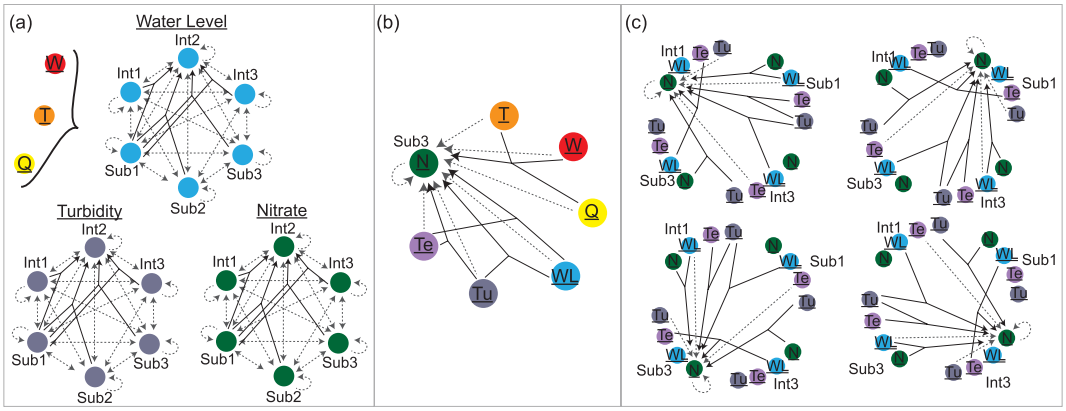

Figure 3. Process networks depicting the three analyses of this work. Line origins are the sources and arrows point toward the target variable. *U* (dashed lines), *R*, and *S* (solid lines) are measured (a) among the locations of the same variable (water level [WL], turbidity [Tu], temperature [Te], and nitrate [N]) to measure connectivity across space, (b) among multiple variables to measure their influence on Sub3-NO_3, and (c) among multiple variables and locations to find the influences on Int1, Int3, Sub1, and Sub3-NO_3. Interactions with external drivers (wind [W], tides [T], and discharge [Q]) are also measured for the first two analyses, and (a) and (b) are also seasonal. Lines in the networks show example relationships.

locations Sub1 ,2, 3, referred to as $R(S)_{Sub}$), among intertidal (locations Int1, 2, 3, higher elevation, $R(S)_{Int}$), and among mixed (e.g., locations Sub1 and Int1, Sub2 and Int3) sources. Finally we compare these *U*, *R*, and *S* values with *R* between each external driver and internal variable (e.g., for tides [T] and WL, we compute $R_{T,WL\rightarrow WL}$) and average over all locations. Relationships for each partition are averaged over the seasons.

The first analysis focuses on the influence of location for each variable. In the second analysis, we use the Oct–Aug data set to measure how the different variables interact to influence Sub3-NO_3 over time (Figure 3b). We compute the seasonal average and maximum *U*, *R*, and *S* relationships among internal variables (all possible combinations of temperature [Te], turbidity [Tu], and water level [WL] at the six locations) and among external variables (discharge, tides, wind [Q,T,W]). We also compare the magnitude of *S* among internal wetland variables to *R* between these variables and external drivers influencing Sub3-NO_3.

For the third analysis, we focus on the influence of variable and location (Figure 3c). The April–Aug data set allows us to capture spatial differences in nitrate dynamics to compare nitrate across various HGM zones. Primary targets of this analysis are Sub1-, Sub3-, Int1-, and Int3-NO_3. Sub2-and Int2-NO_3 are not analyzed as targets as they had significant data gaps. We compute *U*, *R*, and *S* for all possible location and variable combinations and show networks of the strongest location pairs for every variable combination influencing each target averaged over the 131 windows. We also measure the magnitude and timescale of U information provided by all variables to Sub3-NO_3 from fall to summer. U is computed over a 48-h time lag (two diurnal tidal cycles) for each window to find the interaction timescale with Sub3-NO_3. Time lags are not incorporated in the analysis for *R* and *S*.

3. Results

3.1. Connectivity of the Wetland and Influence of External Drivers

Overall, water level is more connected across the island than turbidity or surface water nitrate: R_{WL} is more than double R_{Tu} and R_{NO3} for all seasons suggesting water signals are more strongly synchronized than turbidity or nitrate (Figure 4a, gray bars). This result is expected as water levels in WLD are strongly influenced by tides (Sendrowski & Passalacqua, 2017; Swenson & Sasser, 1993) and water levels are most redundant with tides (boxes in Figure 4a). R_{WL} is greater than $R_{T,WL\rightarrow WL}$, however, suggesting that while each location is tidally influenced, the wetland water level signals are more similar to each other than tides likely due to transport between locations (Figure 4d). Previous studies of WLD using hydrodynamic model simulations suggest that despite the micro-tidal (30 cm) regime in WLD, tides maintain hourly exchange between channels and the wetland along the delta front, even during the spring high river discharge season. This dynamic

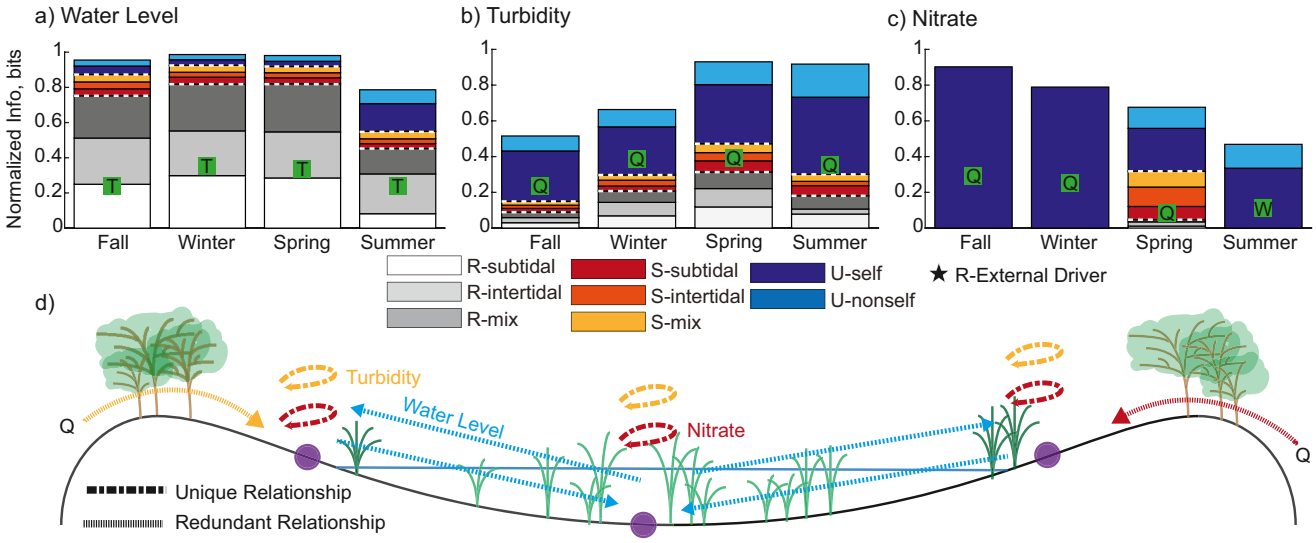

Figure 4. The unique (*U*), synergistic (*S*), and redundant (*R*) information, measured in bits, among (a) water level, (b) turbidity, and (c) nitrate over the four seasons. Overall average *U*, *R*, and *S* relationships are shown in proportion to each other (separated by dashed white lines) and then further partitioned into self and non-self couplings for *U* information (blue bars, top), and into subtidal, intertidal, and mixed sources for *S* (red bars, middle) and *R* (white/gray bars, bottom) information. Total information is normalized for each variable to directly compare water level, turbidity, and nitrate. The letters are the average R between the variable and the strongest external driver (T is tide, Q is discharge, W is wind) for that season. For nitrate relationships in (c), the fall and winter data are from the Oct to Aug data set (where only Sub3-NO_3 data are available), while spring and summer show the Apr–Aug data set where all NO_3 data are available. (d) Conceptual figure showing the strongest relationships from (a) to (c). Dashed lines are U relationships and dotted lines are R relationships. Blue lines refer to water level relationships, orange refers to turbidity, and red refers to nitrate.

forcing results in low water age (the time water from the main river channel spends in the delta wetland) in WLD (Christensen et al., 2020). Similarly, another study in WLD shows strong correlation in water levels between upstream and downstream locations in Mike Island (Elliton et al., 2020). The surface roughness of the wetland (a result of bed roughness or vegetative drag) affects the water level signal such that it further differentiates the water level from external drivers (i.e., decreases $R_{Ext.Driver,WL \rightarrow WL}$).

Seasonal trends in R_{WL} and U_{WL} are influenced by patterns in hydrological connectivity controlled by vegetation coverage and external forcing. Peak hydrological disconnectivity of the wetland occurs during the winter when incoming river discharge is low and many intertidal locations along Mike Island become subaerial for a portion of the window (Figure 5a). Despite this disconnectivity, average R_{WL} (including $R_{Int\text{-}WL \rightarrow WL}$) is consistent from winter to spring likely due to tidal and discharge forcing in winter and spring, respectively. Maximum R_{WL} increases as the spring flood pulse occurs (Figure 1b). The decrease in R_{WL} in summer coincides with an increase in U_{WL}, especially among self-couplings (blue bars in Figure 4a). This trend suggests water level variations are more locally controlled during summer, which we attribute to increasing vegetation coverage that presents a physical barrier to flow, affecting process connectivity of the wetland. Sendrowski and Passalacqua (2017) found similar results for a study on multiple islands in WLD where wind-driven process connections persisted as hydrological connectivity was maintained, but connections were diminished as vegetation coverage increased. Similarly, experimental model simulations in WLD indicate that the presence of wetland vegetation (modeled as increased bed roughness) decreases hydrological connectivity of the delta by preventing water flow into the floodplain (Hiatt & Passalacqua, 2017).

Turbidity fluctuations are influenced by river discharge and the local surface. R_{Tu} is highest in winter and spring (Figure 4b), as discharge increases synchronization among turbidity signals. $R_{Q,Tu \rightarrow Tu}$ (boxes in Figure 4b) is greater than R_{Tu} for all seasons suggesting that river discharge, rather than the local sediment transport processes, drives similarity in the turbidity signal across all locations. This finding is supported by U_{Tu} information; U_{Tu} is stronger for self-couplings (Figure 4b) further suggesting a lack of sediment transport between locations. Local conditions, such as wetland surface roughness, may shorten transport distances compared to water and cause each site to exhibit a memory effect (Figure 4d). However, in winter,

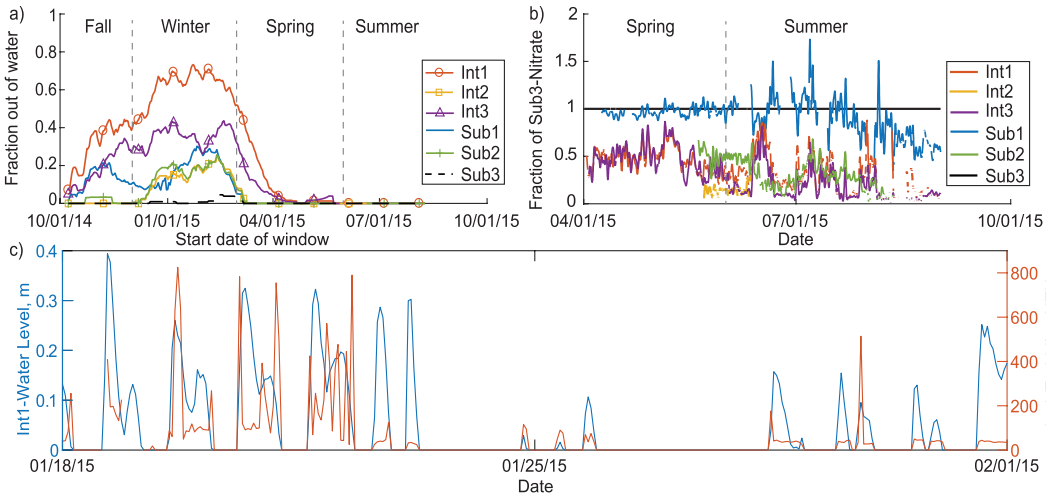

Figure 5. (a) The fraction of time each sensor was not inundated for every window of analysis for the Oct–Aug data set. (b) Observations of nitrate collected at the six locations for the Apr–Aug data set. The nitrate signal was low-pass filtered to remove fluctuations <30 h. Nitrate is plotted here as a fraction of filtered Sub3-Nitrate. (c) Time series observations of water level (blue) and turbidity (orange) at location Int1 for the period 01/18–02/01 2015.

when vegetation dies off, sediment transport distances may lengthen. Strong turbidity fluctuations observed during winter tidal inundation periods provide some evidence of this phenomenon (Figure 5c).

Surface nitrate dynamics are similar to turbidity results. $R_{Q,NO3 \rightarrow NO3}$ (boxes in Figure 4c) exceeds R_{NO3} suggesting nitrate synchronization is dominated by external drivers. U_{NO3} is the strongest influence on nitrate for all seasons and is strongest for self-couplings. A recent study shows that distinct differences in sediment organic matter content and hydroperiod across HGM and chronosequence zones in Mike Island along with seasonality (i.e., temperature) are key factors controlling benthic nutrient fluxes and nitrate removal rates of deltaic wetlands in this region (S. Li et al., 2020). Consequently, nitrate dynamics are highly localized, as indicated by our findings, which also suggest that nitrate dynamics at each site exhibit a strong memory effect. This result is supported by the stronger S_{NO3} and U_{NO3} compared to R_{NO3} measured in spring (i.e., little synchronization among signals, Figure 4c) and the high variation in nitrate measured at different locations along Mike Island (Figure 5b) reflecting spatial variation in wetland connectivity, vegetation density, and nutrient processing that results in differences in nitrate transport and removal. The decrease in nitrate synergy in summer could be due to greater disconnectivity of the wetland, but more likely is a result of data gaps toward the end of the nitrate data set (Figure 5b).

3.2. Controls on Nitrate Variability Through Time

Here, we explore how other variables influence Sub3-NO_3 over time. As Sub3 is an area of higher hydrological connectivity, we expect strong connections between nitrate and the other variables. We focus on U and S among variables as the relationships are weakly redundant. Internal and external variables more strongly influence Sub3-NO3 synergistically than uniquely. While $U_{Sub3\text{-}NO3 \rightarrow Sub3\text{-}NO3}$ is still the strongest influence on Sub3-NO_3, $S_{QTW \rightarrow Sub3\text{-}NO3}$ is also a strong influence (Figure 6), as Sub3 is structurally connected to the adjacent distributary channel and interdistributary bay, resulting in stronger process connectivity to external drivers. External drivers are more synergistic than redundant as they each influence delta variables over different timescales and magnitudes (Sendrowski & Passalacqua, 2017). Other strong Sub3-NO_3 influences include $S_{WL,Te \rightarrow Sub3\text{-}NO3}$, a hydrological and biogeochemical coupling, and $S_{Te \rightarrow Sub3\text{-}NO3}$ and $S_{Te,Tu \rightarrow Sub3\text{-}NO3}$, biogeochemical couplings. The higher S among temperatures and between temperature and turbidity compared to their R across the wetland reflect their influence on processing rates of Sub3-NO_3, though the mechanisms of these process connections likely change over the seasons. We expected to capture less or weaker process connections in winter as we observe that interior locations become subaerial for 20–70% of windows (i.e., hydrological disconnectivity is high, Figure 5a) and many couplings influencing Sub3-NO_3 weaken from fall to winter (first two networks in Figure 6). Yet some couplings strengthen in winter such as

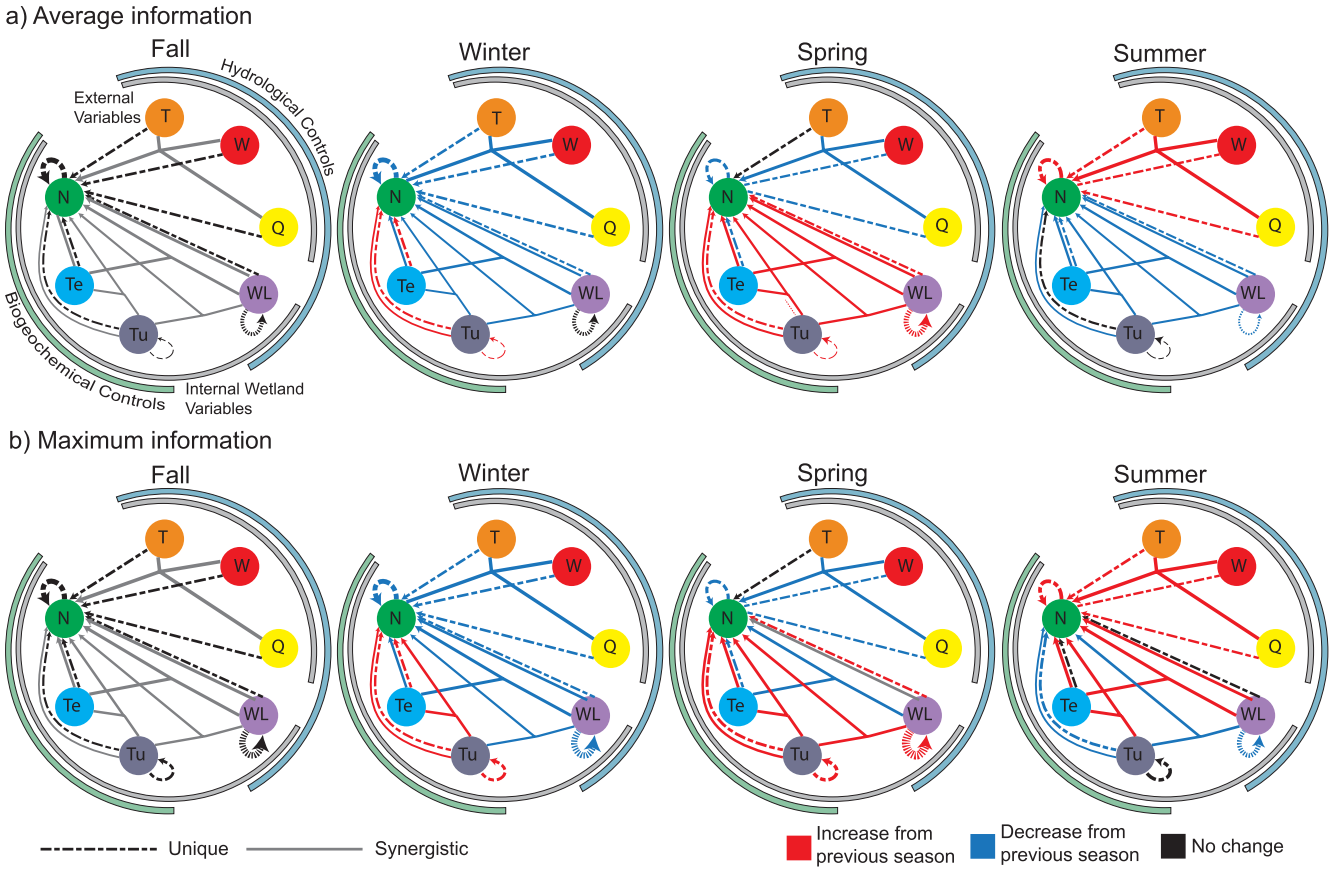

Figure 6. Process networks showing the (a) average and (b) maximum unique and synergistic information relationships that influence Sub3-Nitrate (N in the figure) over the four seasons. Dashed lines show unique information from each variable. Solid lines are the synergistic information provided by each individual internal variable, each internal variable coupling (e.g., water level [WL] and temperature [Te], turbidity [Tu] and water level), and among external drivers (T = tide, W = wind, Q = discharge). Line weights reflect the strength of the relationship. The relationships in winter, spring, and summer are colored for when they increase (red color), decrease (blue), or do not change (black) from the previous season.

maximum $S_{Te,Tu \rightarrow Sub3\text{-}NO3}$ likely due to external driver influence as maximum $R_{QTW,Tu \rightarrow Sub3\text{-}NO3}$ and average $R_{QTW,Te \rightarrow Sub3\text{-}NO3}$ exceed $S_{Te,Tu \rightarrow Sub3\text{-}NO3}$ (Figure 7). We hypothesize that nitrate variability at this location is less likely driven by removal (denitrification) given this dependency with external drivers and the lower temperatures in winter that inhibit benthic fluxes (S. Li et al., 2020).

While external variables drive process connections in winter and spring, we propose vegetation drives them in summer. Spring floods increase hydrological connectivity of the wetland coinciding with strengthened process couplings affecting nitrate (third network in Figure 6). The 2015 spring flood lasted several months into the summer, and yet despite continuous inundation (Figure 5a), process couplings influencing nitrate weaken in summer, and many variables experience strengthened self-uniqueness, which suggests local-scale controls on variable fluctuations (Figures 4 and 6). Previous studies in WLD found that vegetation can promote hydrological disconnectivity and increasingly confine flow into channels (Christensen et al., 2020; Hiatt & Passalacqua, 2017) which may decrease the occurrence of process connections between locations (Sendrowski & Passalacqua, 2017). However, the presence of vegetation also increases the hydraulic residence time, which may increase process couplings at a single location or between variables dependent on the longer contact time. The average strength of couplings weakens during the growing season in agreement with previous research, while maximum information increases for most wetland couplings (and R with external drivers decreases, Figure 7), suggesting longer hydraulic residence times could be increasing process connections at certain locations or between certain variables and we explore this further in the next section.

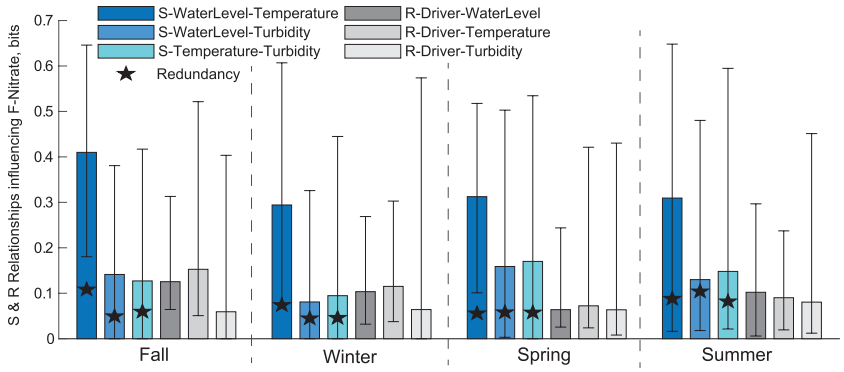

Figure 7. Average *R* and *S* information influencing Sub3-NO_3 over the four seasons. The first three bars (in shades of blue) for each season represent average *S* among water level, temperature, and turbidity, while the next three bars (in shades of gray) are the average *R* between external drivers (averaged for tides, wind, and discharge) and water level, temperature, and turbidity, respectively. Lines on bars are the maximum and minimum values of the relationship. Stars are the average *R* for the wetland coupling.

3.3. Hotspots and Functional Zones of Nitrate Processing

Given the spatial dependence of nitrate removal related to organic matter content, hydroperiod, and temperature, we now measure the influence of different variables and HGM zones on nitrate. We first compute the unique influence of all variables on Sub3-NO_3 and measure their interaction timescale; this timescale represents an information flow timescale, first quantified in WLD and connected to water transport timescales by Sendrowski and Passalacqua (2017). The timescales for $U_{\text{ExternalDrivers}\rightarrow \text{WL}}$ in this analysis (not shown) are similar to their results, suggesting that the lag values provide a similar insight into variable dependency. Unique influence from the other locations is comparable to the influence from Sub3 variables (Figure 8), however, the timescales of these relationships are different across space and change over the seasons. For example, the magnitude of $U_{\text{Te}\rightarrow\text{Sub3-NO3}}$ is similar for all locations and $U_{\text{Sub1-WL}\rightarrow\text{Sub3-NO3}}$ is similar to $U_{\text{Sub3-WL}\rightarrow\text{Sub3-NO3}}$, but the timescale of $U_{\text{Sub3-Te}\rightarrow\text{Sub3-NO3}}$ lengthens from winter to summer (Figure 8b and 8d) as does $U_{\text{WL}\rightarrow\text{Sub3-NO3}}$ for most locations. This shift coincides with strengthened S among some internal variables influencing Sub3-NO_3 (Figure 6). The higher $U_{\text{WL}\rightarrow\text{Sub3-NO3}}$ timescales we measure suggest increased vegetation coverage is lengthening the hydraulic residence time and causing an increase in process connection strength. The increased contact time leads to stronger interactions between wetland variables that biogeochemically influence nitrate (Kadlec, 2010) such that we measure increased $S_{\text{WL,Te}\rightarrow\text{Sub3-NO3}}$. Numerical modeling results of WLD show that, while increased vegetation density decreases overall hydrological connectivity, it increases water exposure time within the wetlands in the delta (Hiatt et al., 2018). Previous work also shows nitrate removal rates in Mike Island are higher in summer than spring likely due to a combination of higher input of riverine nitrate and higher ambient temperature during the summer, suggesting that temperature and turbidity couplings are driven by local wetland processes such as the interaction of warmer temperatures with benthic organisms and organic matter content in soils (influenced by turbidity) that act on nitrate (S. Li et al., 2020).

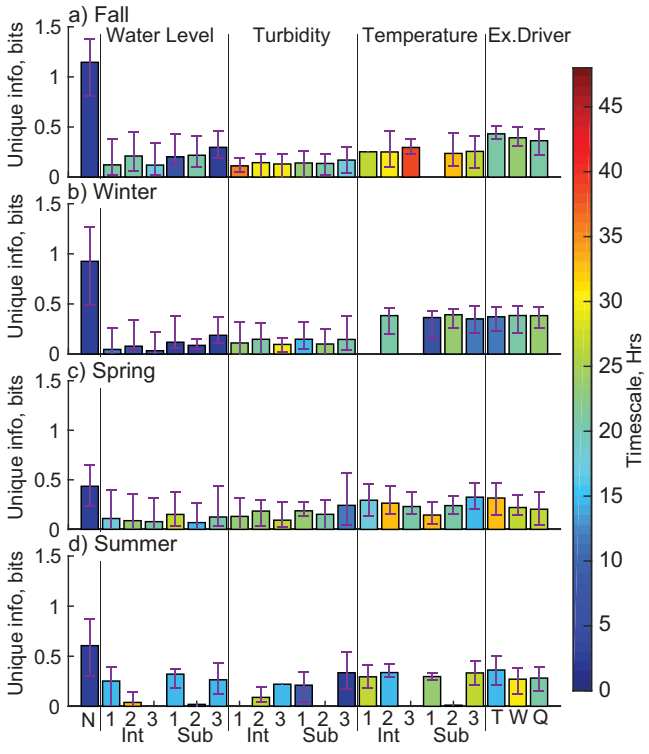

Figure 8. Average unique information provided to Sub3-NO_3 (N) from water level, turbidity, and temperature at all locations along with discharge (Q), tides (T), and wind (W) for (a) fall, (b) winter, (c) spring, and (d) summer. Lines on bars are the maximum and minimum values of the relationship. Colors are the timescale of interaction found at the lag of maximum mutual information for each variable on Sub3-NO_3. The horizontal axis refer to the location for water level, turbidity, and temperature.

Viewing the spatial extent of U and S relationships influencing Sub1, Int1, Int3, and Sub3-NO_3, we find the specific hotspots and zones that emerge to influence NO_3 across locations. Interestingly, while we observe

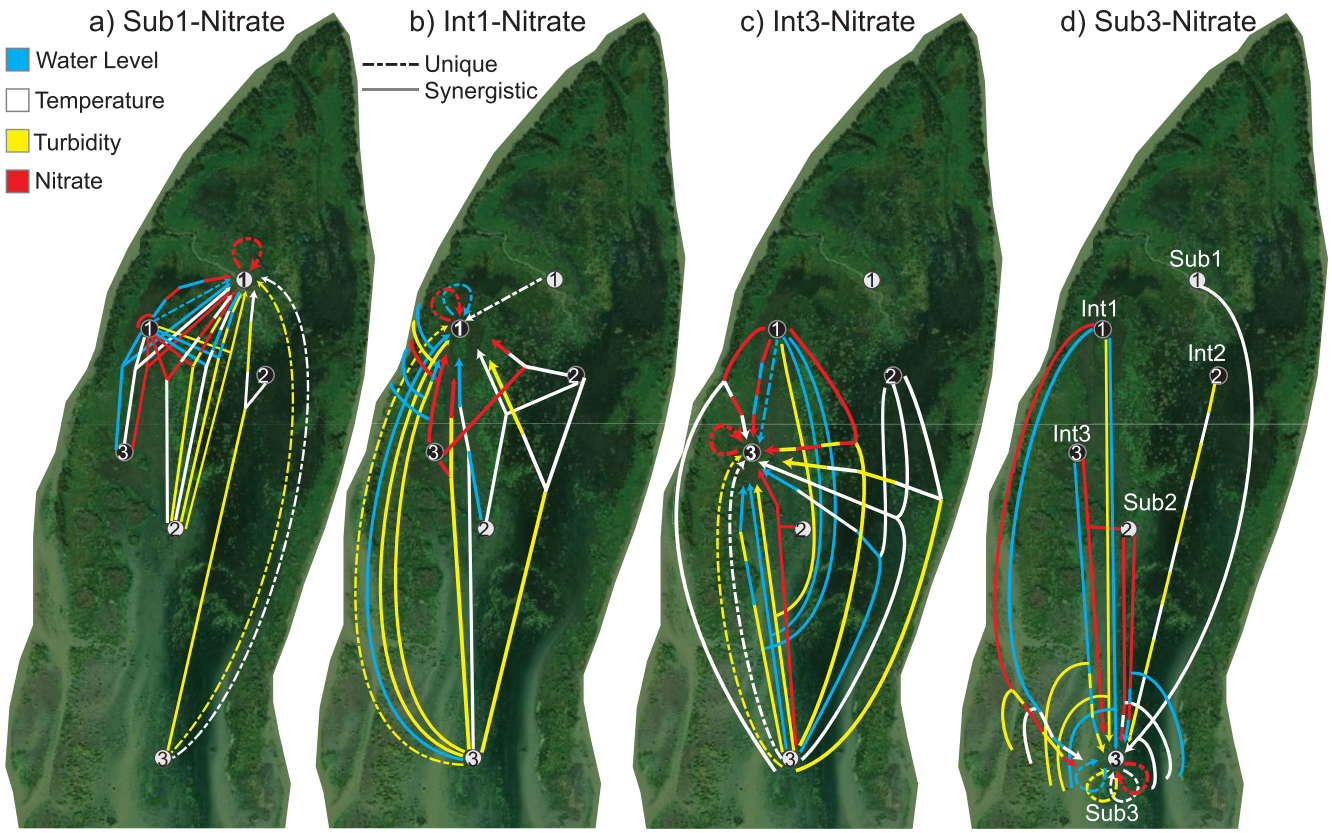

Figure 9. Process networks showing the sources of the maximum unique and synergistic couplings of all internal variables influencing (a) Sub1, (b) Int1, (c) Int3, and (d) Sub3-Nitrate. Unique information is shown as a dashed line and synergistic relationships are solid lines. The line color distinguishes the variables of water level (blue), temperature (white), turbidity (yellow), and nitrate (red). Loops or curved lines close to the target indicate that the location influences itself. For example, the strongest source of nitrate unique information to Sub3-Nitrate is itself (red loop in [d]) and the maximum synergy of turbidity and water level on Sub3-Nitrate is between Sub3-Turbidity (yellow solid line) and Int3-Water Level (blue line). Images of Mike Island copyright 2017 Digital Globe, Inc.

lengthened $U_{\text{Sub3-WL}\rightarrow\text{Sub3-NO3}}$ and $U_{\text{Sub3-Te}\rightarrow\text{Sub3-NO3}}$ timescales from winter to summer, we measure shortening interaction timescales for $U_{\text{Sub3-Tu}\rightarrow\text{Sub3-NO3}}$ and $U_{\text{Int2-Te}\rightarrow\text{Sub3-NO3}}$ and the strongest sources of turbidity and temperature information generally emerge from locations Sub3 and Int2, respectively (Figure 9). Sub1-NO_3 is influenced by five S couplings from locations Int1 and Sub2, where Sub2-Te and Sub2-Tu interact with Int1-WL and Int1-NO_3 to inform on fluctuations at Sub1 (Figure 9a). Int3-NO_3 is influenced by relationships between locations Int1 and Sub3 and Int2 and Sub3. Less influence is measured from location Sub2, despite the proximity of Int3 and Sub2. The zones that emerge may represent physical flow paths that develop in between vegetation patches as overall hydrological connectivity of the wetland decreases (i.e., flow is occurring from Int1 and Sub2 to Sub1 but not between Int3 and Sub2 due to vegetative barriers) or they may represent "information areas" that contain processing information that reduces uncertainty in variable fluctuations. For example, Int2-Te more strongly synergizes with other variables to influence NO_3 compared to temperature at the location of interest. The features at Int2 in the intertidal zone (such as sediment organic matter content, average summer temperature, and hydroperiod) may result in faster processing rates of NO_3 at Int2 = (and Int2 has the lowest nitrate concentrations of all areas studied suggesting nitrate removal is occurring [Figure 5]) and this informs on future processing at the other locations; thus location Int2 is a hotspot of temperature information.

Nitrate is not generally influenced by variables within the same HGM zone and the strongest couplings are measured across HGM zones. Given the complexity of wetland structure and biogeochemical processing in WLD, it is likely that the wetland is a mix of physical preferential flow paths (flow moving across HGM zones) and information areas (information within HGM zones) that interact to influence NO_3 dynamics. The functional zones that we measure suggest that flow and information flow in this system are moving

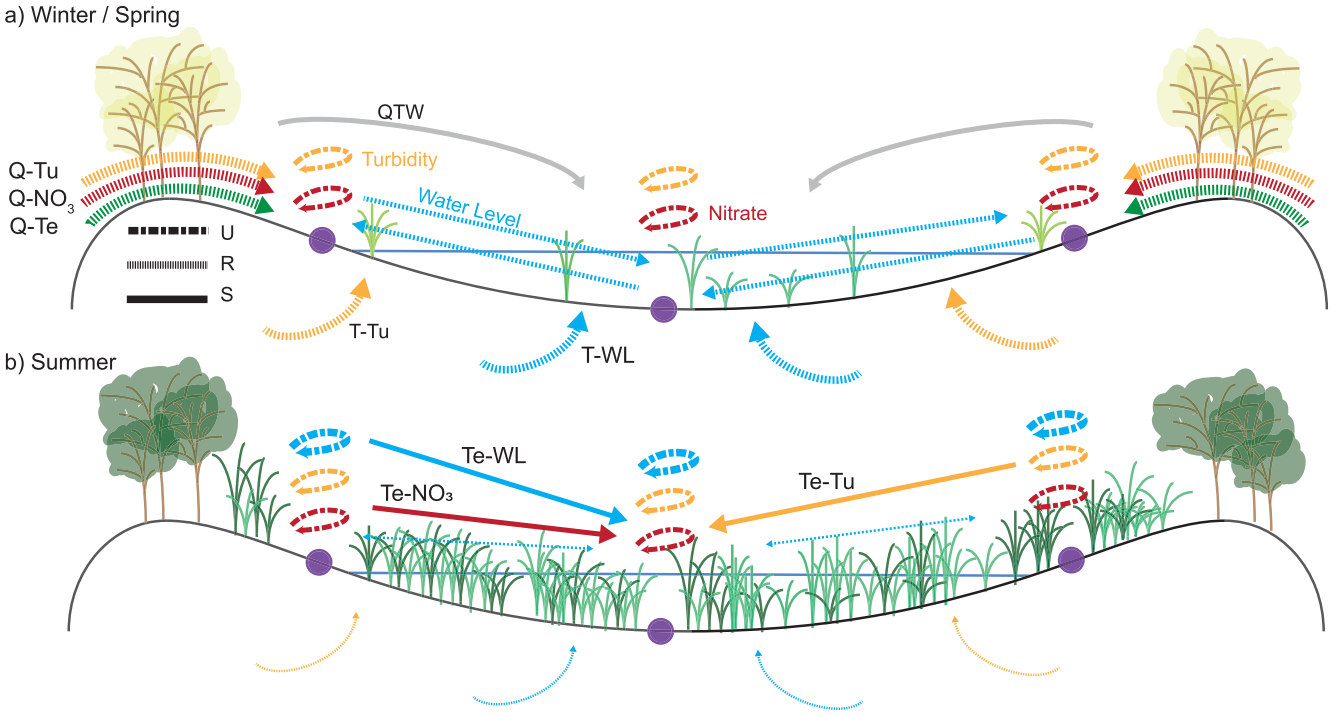

Figure 10. Conceptual figures showing the overall difference in process connections between (a) winter and spring and (b) summer. Dashed lines are *U* relationships, dotted lines are *R* relationships, and solid lines are S relationships, with variables labeled in the figure. Q = discharge, T = tide, Te = temperature, Tu = turbidity, W = wind, WL = water level.

upstream in this period. Location Sub1 variables are not strong sources of information despite their location in the subtidal zone at the end of a secondary channel. Nitrate is most influenced by variables located downstream of it. The emergence of dense vegetation patches across the wetland may prevent downstream movement of flow, while tides, a persistent forcing in this system, would assist in delivering material up-island. This result explains how location Sub3 is a hotspot of influence as it likely maintains physical flow connections and may serve as an information area as well.

4. Discussion

4.1. Mechanisms Maintaining Process Connectivity in Deltaic Wetlands

Throughout the period of study, Mike Island experienced variation in vegetation patterns, seasonality, and external driver forcings. These mechanisms affected the magnitude and timing of variable fluctuations, which result in differences in process connectivity measured across the wetland. In winter and spring, wetland variables that influence Sub3-NO_3 were highly synchronized with external drivers, including temperature. These drivers acted together to deliver material in the wetland, which had lower surface roughness due to a lack of vegetation (Figure 10a). Water levels were also highly redundant in this time, suggesting transport was occurring across the wetland. These results suggest that nitrate fluctuations were transport-dominated during this period, captured as stronger hydrological controls on nitrate compared to biogeochemical controls. A caveat here is that we only had nitrate measurements for one location from fall to spring. The low redundancy among nitrate signals in the April–Aug data set (Figure 4c) suggests that findings for one location may not be extrapolated across space, thus future work should focus on capturing these dynamics at multiple locations in WLD.

In contrast, in summer we measured strengthened relationships among wetland variables as their redundancy with external drivers decreased. Variable fluctuations also showed more local controls, as surface roughness of the wetland and hydraulic residence time increased due to vegetation emergence (Figure 10b). The strongest relationships were between temperature and other wetland variables and these patterns were

consistent when analyzed for nitrate at multiple locations, suggesting that nitrate fluctuations are transformation-dominated during this time, captured as stronger biogeochemical process connections despite high hydrological disconnectivity of the wetland.

While the timescales and individual locations that interact to influence nitrate represent site-specific knowledge based on the physical emplacement of sensors in the wetland, the shifts we measure in process connectivity over time are a transition that likely occurs in many systems. The timing and magnitude of this transition are strongly controlled by external drivers and the extent and density of vegetation coverage. Previous work shows that vegetation patterns can significantly influence flow and sediment in wetlands (Ma et al., 2018; Piliouras & Kim, 2019; Piliouras et al., 2017; Wright et al., 2018) and are linked to insights into nitrate removal (Knights et al., 2020), making vegetation a driving mechanism on transitions in hydrological and biogeochemical process connections.

Older intertidal HGM zones with high sediment organic matter content are the most efficient sites for nitrate removal. Pevious work indicates that the annual nitrate removal capacity (via denitrification) of deltaic wetlands in WLD accounts for 10–27% of the total nitrate load to WLD, with over 90% of the annual N removal occurring during warmer temperatures ($>17^{\circ}C$) and higher surface nitrate concentrations. This is particularly significant given that WLD is a young prograding coastal deltaic floodplain where the capacity of N removal increases by 0.2–2% per year, prior to riverine nitrate export to adjacent coastal waters (S. Li et al., 2020). Future studies should look into the transitions in process connectivity more closely and identify conditions that optimize nutrient removal, including measuring process connections within and across HGM zones, especially in older versus younger portions of wetlands where organic matter and nutrient processing can show strong spatial differences (Bevington & Twilley, 2018; Henry & Twilley, 2014; S. Li et al., 2020). The inclusion of other variables such as sediment organic matter content, phosphorus, dissolved oxygen, and dissolved organic carbon in an analysis such as the one performed here would also provide insight into wetland nutrient processing. The approach used in this study and the timescales and locations uncovered can be used to compare numerical modeling results; the differences between field and modeled process connections can provide insight into model development related to nutrient processing (Sendrowski et al., 2018).

4.2. Monitoring Nitrate in a Wetland

We find that the strongest synergistic couplings influencing nitrate tend to occur between variables at an intertidal and subtidal location. This spatial coupling may be a feature of wetland processing dynamics; it is not simply the development of hydrogeomorphic zones, but the exchange of information across these zones that drives nitrate processing in a wetland. The sensors in our study were strategically placed to measure variables in these zones; our results show that location matters when understanding nitrate processing controls and supports the functional descriptions of wetlands based on hydrogeomorphology (Brinson, 1993). The placement of sensors for nutrient monitoring is thus critical to ensure that processes of interest are captured. Rather than placing sensors for a measure of mass inflows and outflows, we propose placing sensors throughout and within different wetland HGM areas to capture process connections, that is, create a budget of the linkages in the system (Dietrich & Dunne, 1978) as was done in this study. This includes sensor placement in areas of known high hydrological connectivity to capture flow paths, and potential areas of lower physical connectivity to capture information areas that may inform on nutrient processing.

4.2.1. Temporal Considerations for Monitoring

This study is unique in that we gathered continuous one-hour measurements of in-situ nitrate and other wetland variables over several months to detect changes in process connections over time. The strongest control was $U_{\text{Sub3-NO3}\rightarrow\text{Sub3-NO3}}$, suggesting that local factors affect the nitrate signal. Variables that may have greater influence on nitrate include organic matter content or temperature at an unmeasured location. Another alternative is that variable interactions occur over a different timescale than was measured here using 21-day windows. This window length may be long enough that some signal interactions are "smoothed out" and the influence of the landscape dominates. To examine this effect, we re-computed the unique information provided to Sub3-nitrate using a 10-day window with a kernel density estimation (KDE) method

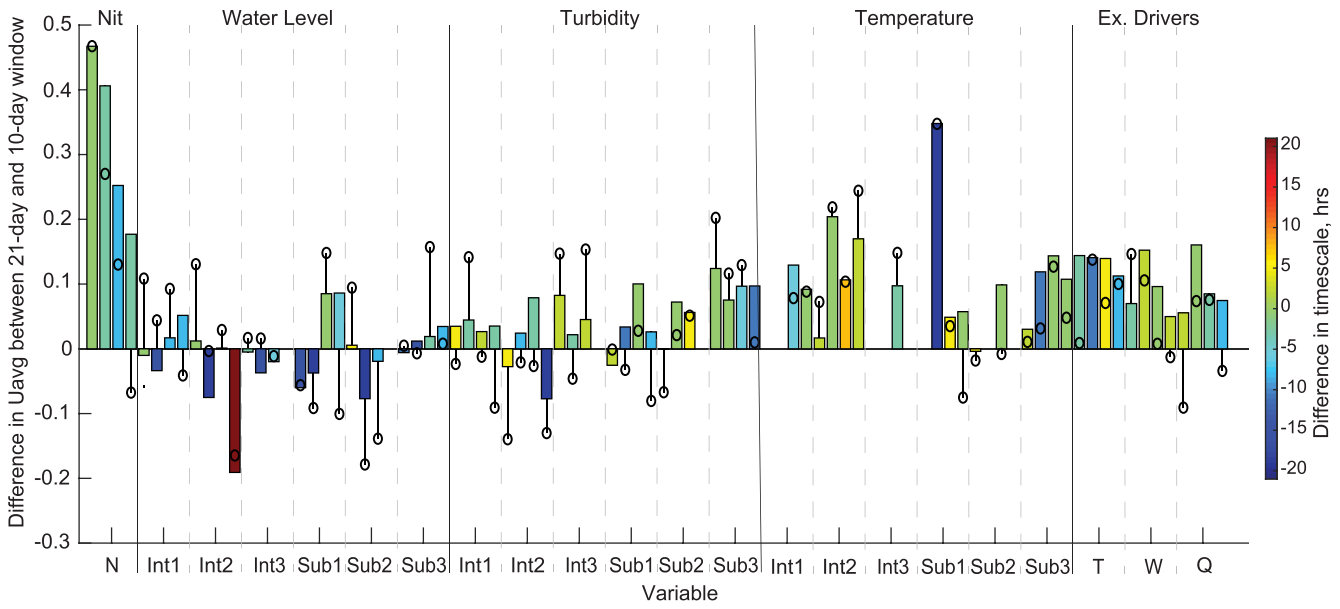

Figure 11. Difference between average (bars) and maximum (circles) unique information found using 21-day windows and 10-day windows for variables influencing Sub3-nitrate over all seasons (seasons shown next to each other in the order fall, winter, spring, summer). Colors of bars are the difference in timescales between the two methods. The horizontal axis refers to the location for water level, turbidity, and temperature. *N* refers to Sub3-Nitrate, Q = discharge, T = tide, W = wind.

(Goodwell & Kumar, 2017b). This method fits a smoothing function to the data and requires less observations to accurately represent the data as a probability density function (Goodwell & Kumar, 2017a, 2017b).

We calculated the difference between (a) the unique information provided to Sub3-nitrate over 21-day and 10-day windows and (b) their interaction timescale (Figure 11). For all seasons, average $U_{\text{Sub3-NO3}\rightarrow\text{Sub3-NO3}}$ found using 21-day windows exceeds the 10-day window value, suggesting that over 10 days nitrate variability may be better explained by other processes beyond previous local fluctuations. One such process includes influence of water level, which shows higher $U_{\text{WL}\rightarrow\text{Sub3-NO3}}$ using 10-day windows, especially in winter, when tidal flushing is occurring over diurnal timescales. External drivers are more persistent forces such that $U_{\text{Ex.Driver}\rightarrow\text{Sub3-NO3}}$ is higher in the 21-day windows (i.e., the smaller fluctuations in tide and wind signals are smoothed out and longer-term patterns, such as the spring-neap tidal cycle, dominate unique external influence on nitrate). When we consider maximum U information, $U_{\text{Tu}\rightarrow\text{Sub3-NO3}}$ and $U_{\text{Sub3-NO3}\rightarrow\text{Sub3-NO3}}$ in summer show stronger influence over 10-day windows (circles in Figure 11) suggesting some locations act over shorter timescales. Despite these differences, the timescales of interaction for most relationships are similar between the two window lengths, suggesting that this timescale is less influenced by window size, an effect which Sendrowski and Passalacqua (2017) saw in their work on window length and mutual information timescales.

Even though the timestep was not shortened, the smaller window results lead to our suggestion that measurement of sub-hourly nitrate fluctuations should be considered. Collecting data over timesteps of 15 or 30 min would allow for a similar analysis to this study over shorter windows and better capture transport across a deltaic island. Transport between locations in Mike Island likely occurred over short time periods due to the small area of the wetland and the high degree of hydrological connectivity.

5. Conclusions

This analysis thoroughly examines the interactions governing nitrate variability in a wetland. Our results reveal mechanisms that likely influence nitrate in many systems and highlight wetland processing characteristics specific to Mike Island. Nitrate controls were analyzed by classifying variable interactions among internal wetland variables and external hydrological drivers using IT statistics. Variables measured at different locations were distinguished by whether they uniquely, synergistically, or redundantly influenced

nitrate variability. The distinct influence of wetland variables was elucidated, along with knowledge of relevant timescales of information flow. The wetland surface roughness, dynamics of external hydrological drivers, seasonality of vegetation, and location in the wetland based on HGM zone are major drivers of nitrate transport and transformation. The results of this work provide a framework for analyzing system linkages that capture the processes of interest that can be used in monitoring and numerical modeling studies related to nutrient processing. We draw the following conclusions:

1. Process connectivity among variables is maintained in winter due to redundancy with external drivers and is maintained in summer due to increased vegetation density that lengthens the hydraulic residence time resulting in increased synergy among biogeochemical variables.
2. Water is more connected across the wetland than turbidity or nitrate, suggesting shorter sediment transport distances and local processing of nitrate fluctuations.
3. Functional zones that influence nitrate form across hydrogeomorphic zones, while temperature hotspots of nitrate influence form in locations with enhanced nitrate processing. Turbidity hotspots form in locations with higher structural connection to the adjacent distributary channel.
4. Specific process couplings that influence nitrate include synergy between temperature and water, among external drivers, and unique local nitrate information.

Data Availability Statement

The discharge data are available at the USGS website, https://waterdata.usgs.gov/nwis/uv?site_no=07381590. The wind and tide data can be downloaded from the NOAA Tides and Currents site for the Lawma-Amerada pass station, https://tidesandcurrents.noaa.gov/waterlevels.html?id=8764227. The information partitioning software can be accessed at https://zenodo.org/badge/latestdoi/73230010. The station data are available through the following: Christensen et al. (2021a, 2021b, 2021c).

Acknowledgments
This material is based on work supported by NSF grants CAREER/EAR-1350336 awarded to P. Passalacqua, FESD/EAR-1135427 awarded to P. Passalacqua. and R. Twilley, Louisiana Sea Grant College Program under NOAA grant NA14OAR4170099 awarded to R. Twilley, and NSF GRFP under grant DGE-1110007 awarded to A. Sendrowski. The authors thank David Mohrig and Wonsuck Kim for their feedback and insights. We also thank the editor, Dr. Goni, and two anonymous reviewers for their constructive comments that helped greatly improve the manuscript.

References

Bevington, A. E., & Twilley, R. R. (2018). Island edge morphodynamics along a chronosequence in a prograding deltaic floodplain wetland. *Journal of Coastal Research*, *34*(4), 806–817. https://doi.org/10.2112/JCOASTRES-D-17-00074.1

Bevington, A. E., Twilley, R. R., Sasser, C. E., & Holm, G. O. (2017). Contribution of river floods, hurricanes, and cold fronts to elevation change in a deltaic floodplain, northern Gulf of Mexico, USA. *Estuarine, Coastal and Shelf Science*, *191*, 188–200. https://doi.org/10.1016/j.ecss.2017.04.010

Bowden, W. B. (1987). The biogeochemistry of nitrogen in freshwater wetlands. *Biogeochemistry*, *4*(3), 313–348. https://doi.org/10.1007/bf02187373

Boynton, W., Hagy, J., Cornwell, J., Kemp, W., Greene, S., Owens, M., et al. (2008). Nutrient budgets and management actions in the Patuxent River Estuary, Maryland. *Estuaries and Coasts*, *31*(4), 623–651. https://doi.org/10.1007/s12237-008-9052-9

Bracken, L. J., & Croke, J. (2007). The concept of hydrological connectivity and its contribution to understanding runoff-dominated geomorphic systems. *Hydrological Processes*, *21*(13), 1749–1763. https://doi.org/10.1002/hyp.6313

Bracken, L. J., Wainwright, J., Ali, G. A., Tetzlaff, D., Smith, M. W., Reaney, S. M., & Roy, A. G. (2013). Concepts of hydrological connectivity: Research approaches, pathways and future agendas. *Earth-Science Reviews*, *119*, 17–34. https://doi.org/10.1016/j.earscirev.2013.02.001

Brinson, M. (1993). Changes in the functioning of wetlands along environmental gradients. *Wetlands*, *13*(2), 65–74. https://doi.org/10.1007/BF03160866

Burt, T. P., & Pinay, G. (2005). Linking hydrology and biogeochemistry in complex landscapes. *Progress in Physical Geography*, *29*(3), 297–316. https://doi.org/10.1191/0309133305pp450ra

Caffrey, J. M., & Day, J. W. (1986). Control of the variability of nutrients and suspended sediments in a gulf coast estuary by climatic forcing and spring discharge of the Atchafalaya River. *Estuaries*, *9*(4), 295–300. https://doi.org/10.2307/1352101

Carle, M. V., & Sasser, C. E. (2016). Productivity and resilience: Long-term trends and storm-driven fluctuations in the plant community of the accreting Wax Lake Delta. *Estuaries and Coasts*, *39*(2), 406–422. https://doi.org/10.1007/s12237-015-0005-9

Christensen, A., Castaneda, E., & Twilley, R. (2021a). Hydrology Data at Wax Lake Delta Observatory (6 stations) - Oct 2014–Aug 2015. *FigShare*. https://doi.org/10.6084/m9.figshare.13100429.v3

Christensen, A., Castaneda, E., & Twilley, R. (2021b). Nitrate Data at Wax Lake Delta Observatory (1 station) - Oct 2014–April 2015. *FigShare*. https://doi.org/10.6084/m9.figshare.13052057.v3

Christensen, A., Castaneda, E., & Twilley, R. (2021c). Nitrate Data at Wax Lake Delta Observatory (6 stations) - April–August 2015. *FigShare*. https://doi.org/10.6084/m9.figshare.13050899.v3

Christensen, A., Twilley, R., Willson, C., & Castañeda-Moya, E. (2020). *Simulating hydrological connectivity and water age within a coastal deltaic floodplain of the Mississippi River DeltaxEstuarine, Coastal and Shelf Science*. Retrieved from http://www.sciencedirect.com/science/article/pii/S0272771420307265

Diaz, R. J., & Rosenberg, R. (2008). Spreading dead zones and consequences for marine ecosystems. *Science*, *321*(5891), 926–929. https://doi.org/10.1126/science.1156401

Dietrich, W., & Dunne, T. (1978). Sediment budget for a small catchment in a mountainous terrain. *Zeitschrift fur Geomorphologie, Supplementband*, *29*, 191–206.
Elliton, C., Xu, K., & Rivera-Monroy, V. H. (2020). The Impact of Biophysical Processes on Sediment Transport in the Wax Lake Delta (Louisiana, USA). *Water (Switzerland)*, Vol. *12*, 2072. https://doi.org/10.3390/w12072072
Geleynse, N., Hiatt, M., Sangireddy, H., & Passalacqua, P. (2015). Identifying environmental controls on the shoreline of a natural river delta. *Journal of Geophysical Research: Earth Surface*, *120*(5), 877–893. https://doi.org/10.1002/2014JF003408
Goodwell, A. E., & Kumar, P. (2017a). Temporal information partitioning: Characterizing synergy, uniqueness, and redundancy in interacting environmental variables. *Water Resources Research*, *53*(7), 5920–5942. https://doi.org/10.1002/2016WR020216
Goodwell, A. E., & Kumar, P. (2017b). Temporal Information Partitioning Networks (TIPNets): A process network approach to infer ecohydrologic shifts. *Water Resources Research*, *53*(7), 5899–5919. https://doi.org/10.1002/2016WR020218
Goodwell, A. E., Kumar, P., Fellows, A. W., & Flerchinger, G. N. (2018). Dynamic process connectivity explains ecohydrologic responses to rainfall pulses and drought. *Proceedings of the National Academy of Sciences of the United States of America*, *115*(37). https://doi.org/10.1073/pnas.1800236115
Hansen, A., Dolph, C., Foufoula-Georgiou, E., & Finlay, J. (2018). Contribution of wetlands to nitrate removal at the watershed scale. *Nature Geoscience*, *11*(2), 127–132. https://doi.org/10.1038/s41561-017-0056-6
Henry, K. M., & Twilley, R. R. (2014). Nutrient biogeochemistry during the early stages of delta development in the Mississippi River Deltaic Plain. *Ecosystems*, *17*(2), 327–343. https://doi.org/10.1007/s10021-013-9727-3
Hiatt, M., Castañeda-Moya, E., Twilley, R., Hodges, B. R., & Passalacqua, P. (2018). Channel-Island connectivity affects water exposure time distributions in a coastal river delta. *Water Resources Research*, *54*(3), 2212–2232. https://doi.org/10.1002/2017wr021289
Hiatt, M., & Passalacqua, P. (2015). Hydrological connectivity in river deltas: The first-order importance of channel-island exchange. *Water Resources Research*, *51*(4), 2264–2282. https://doi.org/10.1002/2014WR016149
Hiatt, M., & Passalacqua, P. (2017). What controls the transition from confined to unconfined flow? Analysis of hydraulics in a coastal river delta. *Journal of Hydraulic Engineering*, *143*(6), 03117003. https://doi.org/10.1061/(ASCE)HY.1943-7900.0001309
Hyfield, E. C. G., Day, J. W., Cable, J. E., & Justic, D. (2008). The impacts of re-introducing Mississippi River water on the hydrologic budget and nutrient inputs of a deltaic estuary. *Ecological Engineering*, *32*(4), 347–359. https://doi.org/10.1016/j.ecoleng.2007.12.009
Kadlec, R. H. (2010). Nitrate dynamics in event-driven wetlands. *Ecological Engineering*, *36*(4), 503–516. https://doi.org/10.1016/j.ecoleng.2009.11.020
Kadlec, R. H. (2012). Constructed marshes for nitrate removal. *Critical Reviews in Environmental Science and Technology*, *42*(9), 934–1005. https://doi.org/10.1080/10643389.2010.534711
Knights, D., Sawyer, A. H., Barnes, R. T., Piliouras, A., Schwenk, J., Edmonds, D. A., & Brown, A. M. (2020). Nitrate removal across ecogeomorphic zones in Wax Lake Delta, Louisiana (USA). *Water Resources Research*, *56*, e2019WR026867. https://doi.org/10.1029/2019wr026867
Lane, R. R., Day, J. W., & Thibodeaux, B. (1999). Water quality analysis of a freshwater diversion at Caernarvon, Louisiana. *Estuaries*, *22*(2), 327–336. https://doi.org/10.2307/1352988
Lane, R. R., Madden, C. J., Day, J. W., & Solet, D. J. (2011). Hydrologic and nutrient dynamics of a coastal bay and wetland receiving discharge from the Atchafalaya River. *Hydrobiologia*, *658*(1), 55–66. https://doi.org/10.1007/s10750-010-0468-4
Lane, R. R., Mashriqui, H. S., Kemp, G., Day, J. W., Day, J. N., & Hamilton, A. (2003). Potential nitrate removal from a river diversion into a Mississippi delta forested wetland. *Ecological Engineering*, *20*(3), 237–249. https://doi.org/10.1016/s0925-8574(03)00043-0
Lexartza-Artza, I., & Wainwright, J. (2009). Hydrological connectivity: Linking concepts with practical implications. *Catena*, *79*(2), 146–152. https://doi.org/10.1016/j.catena.2009.07.001
Li, C., Roberts, H., Stone, G. W., Weeks, E., & Luo, Y. (2011). Wind surge and saltwater intrusion in Atchafalaya Bay during onshore winds prior to cold front passage. *Hydrobiologia*, *658*(1), 27–39. https://doi.org/10.1007/s10750-010-0467-5
Li, S., Christensen, A., & Twilley, R. R. (2020). Benthic fluxes of dissolved oxygen and nutrients across hydrogeomorphic zones in a coastal deltaic floodplain within the Mississippi River delta plain. *Biogeochemistry*, *149*, 115–140. https://doi.org/10.1007/s10533-020-00665-8
Ma, H., Larsen, L. G., & Wagner, R. W. (2018). Ecogeomorphic feedbacks that grow deltas. *Journal of Geophysical Research: Earth Surface*, *123*, 3228–3250. https://doi.org/10.1029/2018JF004706
McClain, M. E., Boyer, E. W., Dent, C. L., Gergel, S. E., Grimm, N. B., Groffman, P. M., et al. (2003). Biogeochemical hot spots and hot moments at the interface of terrestrial and aquatic ecosystems. *Ecosystems*, *6*(4), 301–312. https://doi.org/10.1007/s10021-003-0161-9
Mitsch, W. J., Day, J. W., Zhang, L., & Lane, R. R. (2005). Nitrate-nitrogen retention in wetlands in the Mississippi River Basin. *Ecological Engineering*, *24*(4), 267–278. https://doi.org/10.1016/j.ecoleng.2005.02.005
Mulholland, P. J., Helton, A. M., Poole, G. C., Hall, R. O., Hamilton, S. K., Peterson, B. J., & Thomas, S. M. (2008). Stream denitrification across biomes and its response to anthropogenic nitrate loading. *Nature*, *452*(7184), 202–205. https://doi.org/10.1038/nature06686
Olliver, E. A., & Edmonds, D. A. (2017). Defining the ecogeomorphic succession of land building for freshwater, intertidal wetlands in Wax Lake Delta, Louisiana. Estuarine. *Coastal and Shelf Science*, *196*, 45–57. https://doi.org/10.1016/j.ecss.2017.06.009
Passalacqua, P. (2017). The Delta Connectome: A network-based framework for studying connectivity in river deltas. *Geomorphology*, *277*, 50–62. https://doi.org/10.1016/j.geomorph.2016.04.001
Piliouras, A., & Kim, W. (2019). Delta size and plant patchiness as controls on channel network organization in experimental deltas. *Earth Surface Processes and Landforms*, *44*(1), 259–272. https://doi.org/10.1002/esp.4492
Piliouras, A., Kim, W., & Carlson, B. (2017). Balancing aggradation and progradation on a vegetated delta: The importance of fluctuating discharge in depositional systems. *Journal of Geophysical Research: Earth Surface*, *122*, 1882–1900. https://doi.org/10.1002/2017JF004378
Rabalais, N. N., Turner, R. E., Díaz, R. J., & Justić, D. (2009). Global change and eutrophication of coastal waters. *ICES Journal of Marine Science*, *66*(7), 1528–1537. https://doi.org/10.1093/icesjms/fsp047
Reddy, K. R., Patrick, W. H., & Broadbent, F. E. (1984). Nitrogen transformations and loss in flooded soils and sediments. *CRC Critical Reviews in Environmental Control*, *13*(4), 273–309. https://doi.org/10.1080/10643388409381709
Rivera-Monroy, V. H., Lenaker, P., Twilley, R. R., Delaune, R. D., Lindau, C. W., Nuttle, W., & Castañeda-Moya, E. (2010). Denitrification in coastal Louisiana: A spatial assessment and research needs. *Journal of Sea Research*, *63*(3–4), 157–172. https://doi.org/10.1016/j.seares.2009.12.004
Ruddell, B. L., & Kumar, P. (2009a). Ecohydrologic process networks: 1. Identification. *Water Resources Research*, *45*(3), W03419. https://doi.org/10.1029/2008WR00727910.1029/2008WR007279
Ruddell, B. L., & Kumar, P. (2009b). Ecohydrologic process networks: 2. Analysis and characterization. *Water Resources Research*, *45*(3), W03420. https://doi.org/10.1029/2008WR007280
Selman, M., Greenhalgh, S., Diaz, R., & Sugg, Z. (2008). Eutrophication and hypoxia in coastal areas: A global assessment of the state of knowledge. *WRI Policy Note*, 1–6.

Sendrowski, A., & Passalacqua, P. (2017). Process connectivity in a naturally prograding river delta. *Water Resources Research*, *53*(3), 1841–1863. https://doi.org/10.1002/2016WR019768

Sendrowski, A., Sadid, K., Meselhe, E., Wagner, W., Mohrig, D., & Passalacqua, P. (2018). Transfer entropy as a tool for hydrodynamic model validation. *Entropy*, *20*(1). https://doi.org/10.3390/e20010058

Shaffer, G. P., Sasser, C. E., Gosselink, J. G., & Rejmanek, M. (1992). Vegetation dynamics in the emerging Atchafalaya Delta, Louisiana, USA. *Journal of Ecology*, *80*, 677. https://doi.org/10.2307/2260859

Shaheen, S. M., Rinklebe, J., Frohne, T., White, J. R., & DeLaune, R. D. (2016). Redox effects on release kinetics of arsenic, cadmium, cobalt, and vanadium in Wax Lake Deltaic freshwater marsh soils. *Chemosphere*, *150*, 740–748. https://doi.org/10.1016/j.chemosphere.2015.12.043

Shannon, C. E. (1948). A mathematical theory of communication. *Bell system technical journal*, *27*, 379–423. https://doi.org/10.1002/j.1538-7305.1948.tb01338.x

Shaw, J. B., Mohrig, D., & Wagner, R. W. (2016). Flow patterns and morphology of a prograding river delta. *Journal of Geophysical Research: Earth Surface*, *121*(2), 372–391. https://doi.org/10.1002/2015JF003570

Shaw, J. B., Mohrig, D., & Whitman, S. K. (2013). The morphology and evolution of channels on the Wax Lake Delta, Louisiana, USA. *Journal of Geophysical Research: Earth Surface*, *118*(3), 1562–1584. https://doi.org/10.1002/jgrf.20123

Smirnov, D. A. (2013). Spurious causalities with transfer entropy. *Physical Review E-Statistical Physics, Plasmas, Fluids, and Related Interdisciplinary Topics*, *87*(4), 42917. https://doi.org/10.1103/PhysRevE.87.042917

Swenson, E. M., & Sasser, C. E. (1993). Water level fluctuations in the Atchafalaya Delta, Louisiana: Tidal forcing versus river forcing. *Coastal and Estuarine Studies*, 191.

Tetzlaff, D., Soulsby, C., Bacon, P. J., Youngson, A. F., Gibbins, C., & Malcolm, I. A. (2007). Connectivity between landscapes and riverscapes: A unifying theme in integrating hydrology and ecology in catchment science? *Hydrological Processes*, *21*(10), 1385–1389. https://doi.org/10.1002/hyp.6701

Turner, R. E., & Rabalais, N. N. (1994). Coastal eutrophication near the Mississippi River Delta. *Nature*, *368*(6472), 619–621. https://doi.org/10.1038/368619a0

Turner, R. E., Rabalais, N. N., & Justic, D. (2008). Gulf of Mexico hypoxia: Alternate states and a legacy. *Environmental Science & Technology*, *42*(7), 2323–2327. https://doi.org/10.1021/es071617k

Twilley, R. R., Day, J. W., Bevington, A. E., Castañeda-Moya, E., Christensen, A., Holm, G., et al. (2019). Ecogeomorphology of coastal deltaic floodplains and estuaries in an active delta: Insights from the Atchafalaya Coastal Basin. *Estuarine, Coastal and Shelf Science*, *227*, 106341. https://doi.org/10.1016/j.ecss.2019.106341

Vanzomeren, C. M., White, J. R., & Delaune, R. D. (2013). Ammonification and denitrification rates in coastal Louisiana bayou sediment and marsh soil: Implications for Mississippi river diversion management. *Ecological Engineering*, *54*, 77–81. https://doi.org/10.1016/j.ecoleng.2013.01.029

Williams, P. L., & Beer, R. D. (2010). *Nonnegative decomposition of multivariate information*. arXiv preprint arXiv:1004.2515.

Williams, P. L., & Beer, R. D. (2011). *Generalized measures of information transfer*. arXiv preprint arXiv:1102.1507.

Wright, K., Hiatt, M., & Passalacqua, P. (2018). Hydrological connectivity in vegetated river deltas: The importance of patchiness below a threshold. *Geophysical Research Letters*, *45*(19), 10416–10427. https://doi.org/10.1029/2018gl079183